

Extraction and characterization of regions of interest in biomedical images

Yakov Keselman
Department of Computer Science
Rutgers University
Piscataway, NJ 08855, USA
keselman@paul.rutgers.edu

Evangelia Micheli-Tzanakou
Department of Biomedical Engineering
Rutgers University
Piscataway, NJ 08855, USA
etzanako@biomed.rutgers.edu

Abstract

A system that could serve as a first stage of a two-stage automated biomedical image classification system is presented. The underlying image segmentation algorithm and several region representations are discussed. Provided examples of extracted (robustly and quickly) regions show flexibility and potential of the approach.

1 Introduction

The problem of automated classification of various biomedical images obtained as a result of screening (e.g. X-ray or mammography) can be approached in two stages. During the first stage "regions of interest", i.e. regions whose presence in the image to a large degree affects how the image is later classified, are extracted. During the second stage the extracted regions are analyzed in more detail in terms of their shape, internal properties (e.g. intensity, texture), as well as locations with respect to the image and to other such regions. It is believed that provided both the stages are performed sufficiently accurately, the resulting system could be of great use in many different biomedical applications, including cell identification, mammography, etc.

The previous efforts in the field mostly concentrated on the second stage where various low-level image processing tools (including wavelet and Fourier analysis, neural networks, pattern matching, etc. – see e.g. [6, 7, 10]) were successfully applied. The first stage, related to problems occurring in low-level image understanding, also received some attention, e.g. in [3, 2, 9]. In general such region extracting systems tend to be less automated because the notion of "region of interest" is in many cases problem-dependent and a successful extraction algorithm should incorporate some field-specific knowledge directly. At present such systems mostly offer some means of interaction to improve the often far from perfect initial segmentation of images.

The approach taken for the system to be described also falls into this category. Namely, after an initial segmentation of an image, the user is offered a set of operations on the resulting regions by means of which it is possible to obtain a desirable segmentation in a few steps. Motivations for various components of the system and their descriptions are given below.

2 Methods

2.1 Image Segmentation

The system is capable of working with both gray level (e.g. mammography) and color (e.g. cellular and retinal) images. The ability results from the features of the underlying simple, robust, and diverse *mean shift* clustering algorithm [1] first applied to image segmentation by Comaniciu and Meer [4]. For a detailed account of the algorithm as well as its properties the reader is referred to the above mentioned papers.

The *mean shift* algorithm itself is designed to find *modes* (or centers of the regions of high concentration) of data represented as arbitrary-dimensional vectors. The algorithm, implemented in a *MATLABTM*

environment, proceeds as follows ([4]):

1. Choose a radius for the search window.
2. Choose the initial location (center) of the window.
3. Compute the mean (average) of the data points over the window and translate the center of the window into this point.
4. Repeat step 3 above until translation distance of the center becomes less than a preset threshold.

An illustration of the *mean shift* algorithm is given in Figure 1.

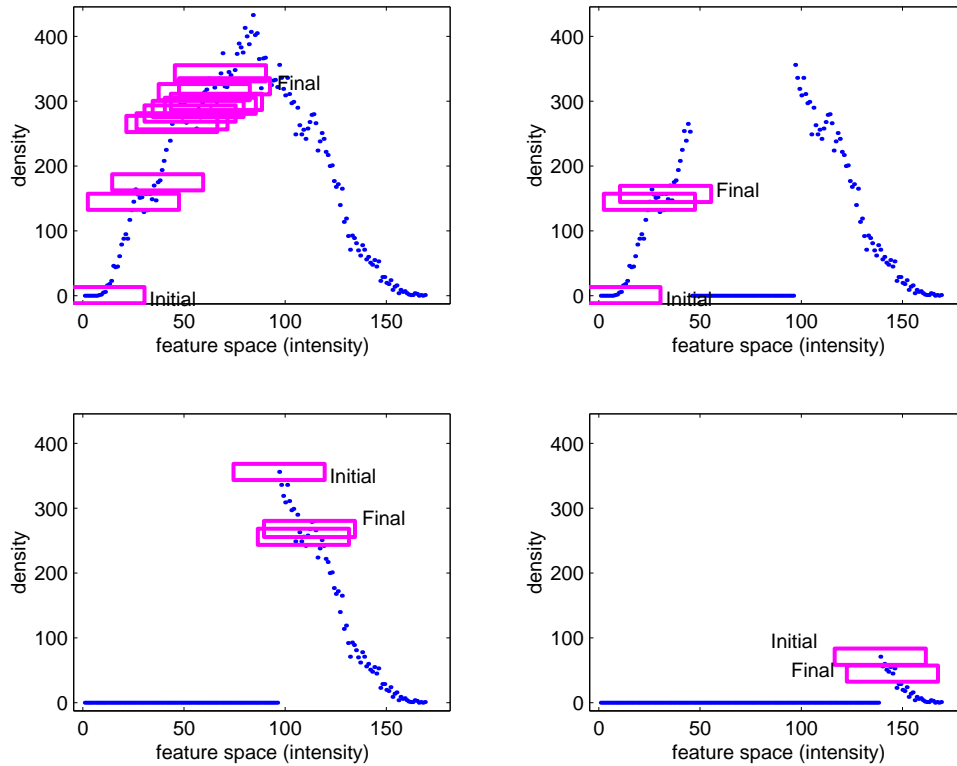


Figure 1: **An illustration of the *mean shift* algorithm.** Initial and final windows of four intensity clusters. Four separate runs of the algorithm are shown. The horizontal axis represents the (one-dimensional) feature space while the vertical axis represents density of vectors.

The algorithm can then be applied to gray level/color segmentation in the following fashion, which is a simplified version of [4]:

1. Map the image domain into the feature space (1-dimensional for gray level images and generally 3-dimensional for color images).
2. Define an adequate number of search windows at random locations in the feature space.
3. Find centers of high density regions by applying the *mean shift* algorithm to each window.
4. Find regions in the image domain corresponding to high density regions in the feature space.

5. Do some postprocessing on the image domain regions based on predefined constraints and prior assumptions.

An illustration of the algorithm adapted for the 2-dimensional case is shown in Figure 2.

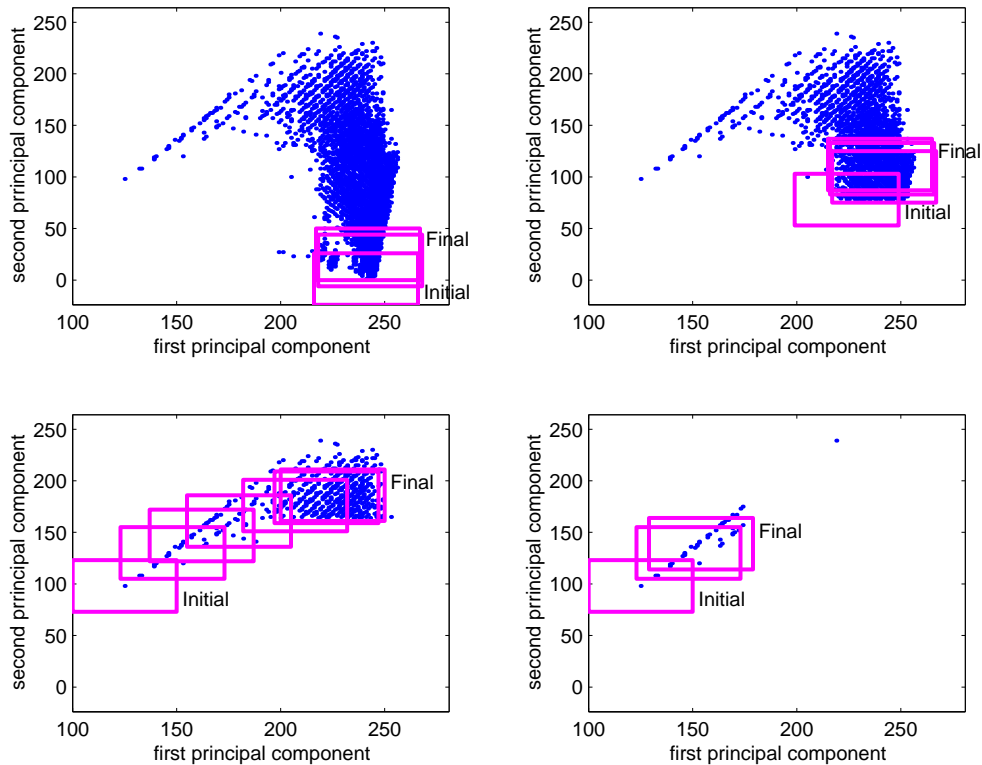


Figure 2: **An illustration of the mean shift algorithm.** Initial and final windows of four point clusters. In this figure, each point represents a pixel in the image encoded in the $L^*u^*v^*$ color space [5]. The axes of the figures can be a representation of two principal components. A random position for the placement of the window is created and the algorithm is applied so that regions of maximum density are found. The window shift is defined by the algorithm. This is accomplished by computing the mean of the data points over the window and translating the center of the window to this point. Four different runs are shown.

Since high density regions in the feature space correspond to sufficiently big numbers of pixels in a narrow range of intensities/colors in the image domain, provided the pixels form connected regions (as is often the case for relatively smooth images), the algorithm essentially finds relatively big connected regions which have sufficiently small variations in intensity/color and thus perceived as well-defined regions by humans as well. In practice, the algorithm proceeds by placing randomly one search window at a time, finding the corresponding mode, and removing all the feature vectors in the final window from the feature space. Thus one would expect to find bigger regions first. Given some a priori information on the image (e.g. lower intensities correspond to background, as it is often the case in mammograms), the strategy could be modified by placing the first window at a preferred position chosen by the user. Provided that additional information about the regions of interest is known (e.g. the regions are characterized by colors rather than their intensities), it could easily be used by the system by applying the same algorithm in a lower-dimensional space.

One of the shortcomings of the segmentation algorithm is that it does not take into account any spatial information at the processing step. This could result in regions with many holes and irregular boundaries due to relatively large variation over a small range of pixels (Figure 3). However depending on prior information



Figure 3: Two possible regions of interest in a mammogram (partial view). The region on the right does not necessarily correspond to a "suspicious" region.

about the image (e.g. that the regions of interest should not have such holes as it is the case for nuclei of cells), such artifacts could be eliminated at the postprocessing stage. The postprocessing stage usually includes such simple morphological operations as removing isolated pixels and small (as defined by the user) regions as well as smoothing boundaries of regions.

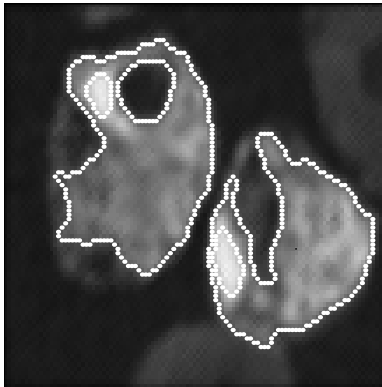


Figure 4: Two extracted contours of cells with not quite satisfactory results. See text for details.

As implemented in the system, after inputting a few parameters, the user obtains an initial segmentation of the image. If the resulting regions are "too small" (as it is the case for the two regions in Figure 4) or "too big" an adjustment of the parameters and resegmentation is required. At present the implementation uses the same window size over the whole spectrum (of values of each color space coordinates), but specification of different window sizes for different parts of spectra could easily be added. In many instances the incoming images are quite far from being smooth (due to low resolution of scanning devices) and a few simple smoothing algorithms (some are plain image filters, and some are wavelet-based) are optionally applied to achieve better segmentation results. In addition, to extract relatively small regions of interest (and to reduce segmentation time) in the image, cropping feature could be used. As another implementation detail, before segmenting color images, pixels, usually represented in the RGB color space, are mapped into the $L^*u^*v^*$ color space (see e.g. [5]) which has a "brightness" component represented by L^* and two "chromatic" components represented by u^* and v^* . It is argued that the latter color space is more isotropic and thus is better suitable for the used Mode finding algorithm. Finally, for efficiency reasons "rectangular" rather than "circular" windows are used. The difference between the two is non-existent for 1-dimensional case and is sufficiently small even for 3-dimensional one.

2.2 Region representations and processing

Provided the initial segmentation is satisfactory, the system allows to work with regions resulting from segmentation. At the moment, regions are assumed to be connected (taking the view that two different regions of about the same intensity/color may be present in the image independently of each other), although the operation of merging allows to form regions consisting of connected subcomponents if desired. In general it is hard to make such decisions at the system level due to the absence of any prior knowledge about the regions nature. If the resulting region encompasses too big a portion of the image and a finer segmentation does not provide satisfactory results (as it might be the case for the region in Figure 5), it is possible to use the included spline-based "Cutting" and "Merging" features to select the region of interest manually.

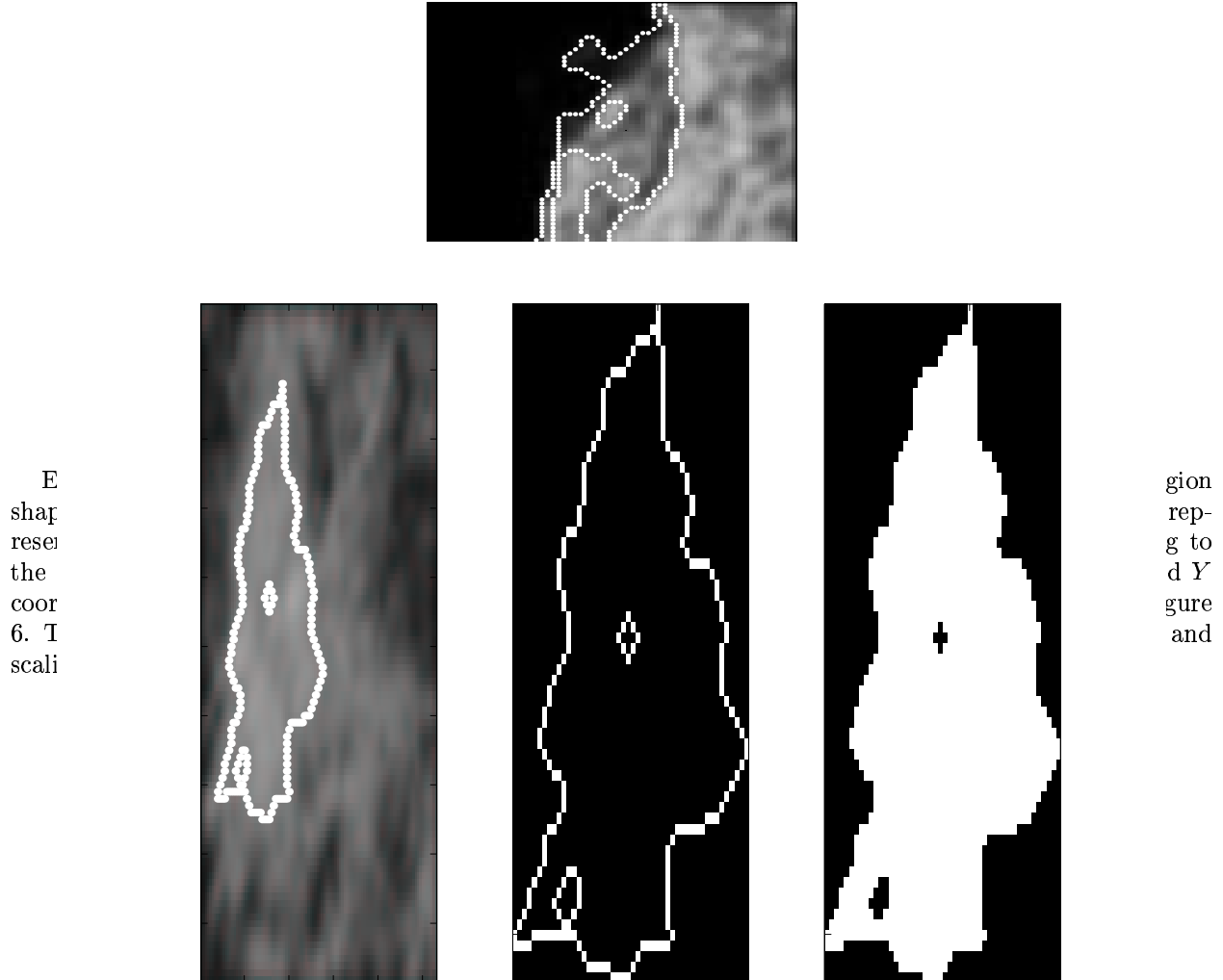


Figure 6: Matrix representation of a region. White pixels in the right two images correspond to ones, and black ones correspond to zeros of the matrices. The image on the right corresponds to the first matrix representation while the image in the middle corresponds to the second matrix representation.

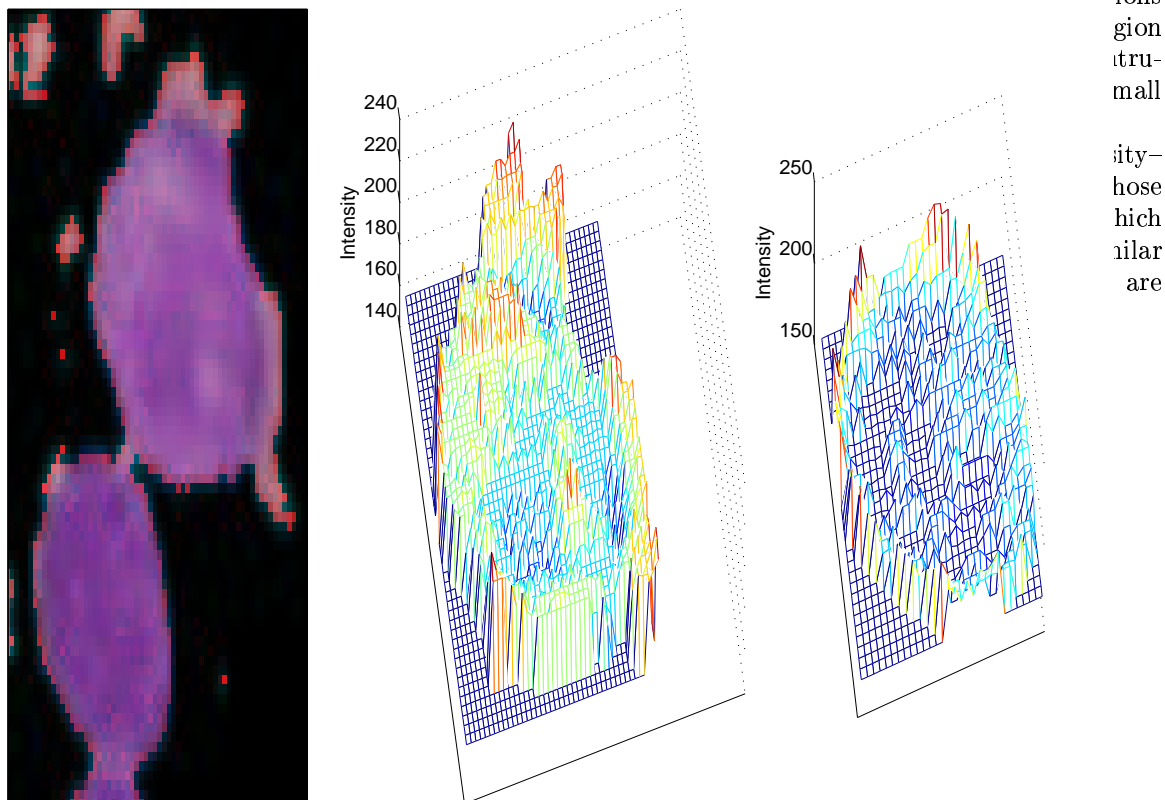
Indeed, assume that the region R_B was obtained from region R_A by replicating each of its pixels over a rectangle of size m by n . Since the rank of matrix B representing region R_B is the same as that of matrix A representing region R_A , the number of non-zero eigenvalues will be the same for both matrices. Also if $\lambda_i(B)$ is the i -th largest eigenvalue of B and $\lambda_i(A)$ is the i -th largest eigenvalue of A , then $\lambda_i(B) = m \cdot n \cdot \lambda_i(A)$.

Since the eigenvalues of a matrix, of its reflection about the central row, and of its transpose coincide, the invariance to rotations by the above angles follows. To accommodate rotations by other angles at the matching step the region is rotated with a fixed step size (e.g. 5° or 10°) and the corresponding eigenvalues are computed. Then the best match is taken. The performed experiments confirmed the applicability of the representation for such rough matching.

Alternatively, regions can be represented by singular values of matrices formed by placing ones only at the boundary pixels of regions. There are advantages and disadvantages to both representations. For example, cutting out a hole in a region will most likely not lead to big changes in the latter representation, provided the boundary of the hole is not very long compared to the boundary of the region (as in Figure 4 in the region on the left), but will likely lead to noticeable changes in the former representation making it more suitable for a more precise shape matching.

An even finer matching could be done by placing not ones, but actual pixel values in the corresponding matrix (or matrices in case of color images) and computing its singular values. An advantage of such representations

is that
conservation:
perturbations
A
base
value
the
region
representation



ions
gion
stru-
mall

ity-
hose
high
ilar
are

Figure 7: 3-dimensional intensity-based representation of two regions. The upper region is represented in the middle while the lower region is represented in the right.

2.3 Extraction of regions of interest – typical steps

Typical steps for extraction of regions of interest are given in Figures 8 – 13 for the particular case of cell image segmentation.

1. Start with the original image and crop/smooth it if necessary.
2. Separate "background" from "foreground" by segmenting the image with a **small window size**.
3. Delete the background from consideration and resegment the image with a **bigger window size**.

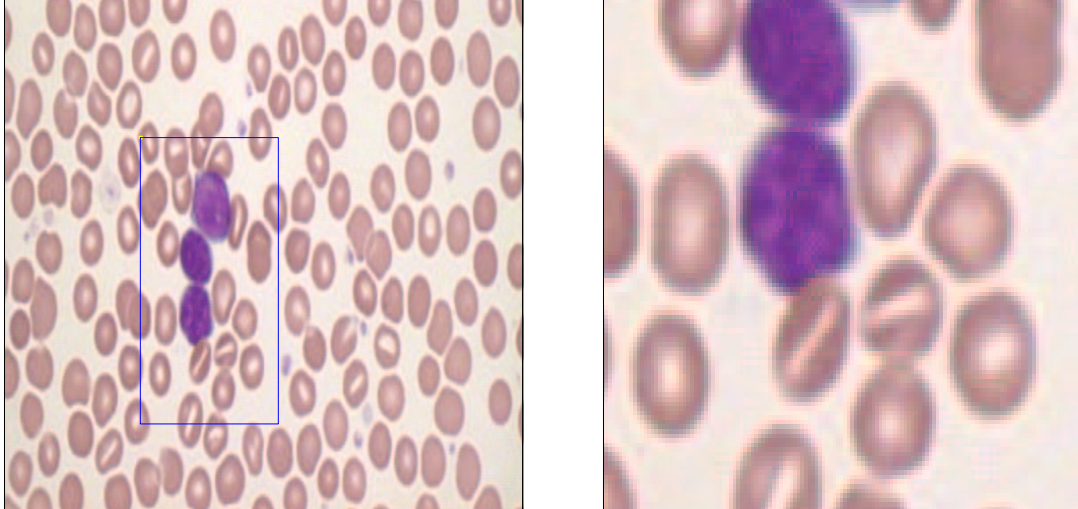


Figure 8: The original image is on the left and its smoothed portion is on the right.

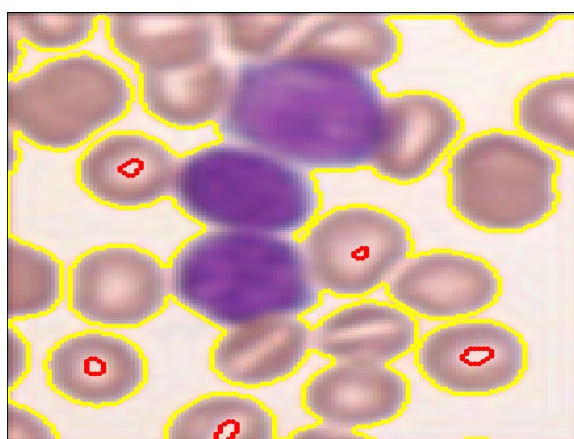


Figure 9: The "background" has yellow boundary. Note small regions in the "foreground" (outlined by red) due to small window size.

4. Perform cutting/merging operations to separate regions if necessary.
5. Visualize and roughly compare regions of interest in a 3-dimensional representation.
6. Compare regions of interest more precisely in terms of their shapes.

3 Applications

In what follows some other applications of the system are illustrated graphically.

3.1 Mammography

Computers can be used in mammography not only to improve detection accuracy but also to improve efficiency. Unlike human beings, computers are objective, do not fatigue, and do not have the limitations of the human visual system. Much research has been invested in computer aided diagnosis of mammograms. For example, computers have been used to enhance mammograms, highlight potential abnormalities, and

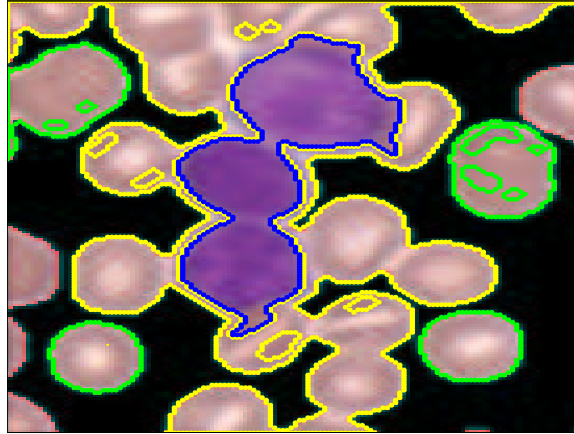


Figure 10: The "background" is now black. Notice that different regions may be grouped together due to large window size.

classify abnormalities as benign or malignant. Finding the regions of interest in mammography is a difficult task, especially if someone wants to do this step applied to the whole mammogram.

The figures below give an example of such a process. A portion of a mammogram (cropped and with "background" removed as described earlier) is shown in 14, while some regions of interest are shown in 15.

Another area in breast cancer is the detection and classification of cells obtained from biopsies. In Figure 16 histological section of breast biopsy specimens containing cancer and matched normal adjacent tissues are shown. Nuclear images are captured with a custom workstation consisting of a CCD camera attached to a bright field microscope and lined to a desktop computer with a frame grabber card.

Images of nuclei are segmented with our new segmentation method that eliminates inter- and intra-observer variation. The segmentation procedure is superior to the methods currently in use by many other laboratories. The new algorithmic segmentation procedure is a combination of edge detection and region growing based on an iterative selection method for thresholding.

Notice the low contrast of the image and the ability of the software to segment background from foreground successfully. Figure 17 shows the same image with background removed and two cells chosen after resegmentation of the image. In Figure 18 the same two cells are represented in 3-dimensional form. They are compared in terms of their shapes, areas, and volumes.

3.2 Retinal image damage from the presence of a tumor

Figure 19 is a representative example of an ultrasound image of a human retina. The outlined region is a suspicious area.

In Figure 20 on the left the tumor has been outlined manually while on the right the automatic outlining is shown. The red area underneath the tumor has been excluded since our method is based on color content as well. If the user wants to include that area, it can be easily done by selecting that region and merging it with the outlined one.

4 Discussion

The system provides a nice graphical user interface to all its functionality and could be easily extended in several directions, including using different image segmentation algorithms, color spaces, and region representations. It processes images in a variety of formats (including "bmp", "jpeg", "tiff"). To increase

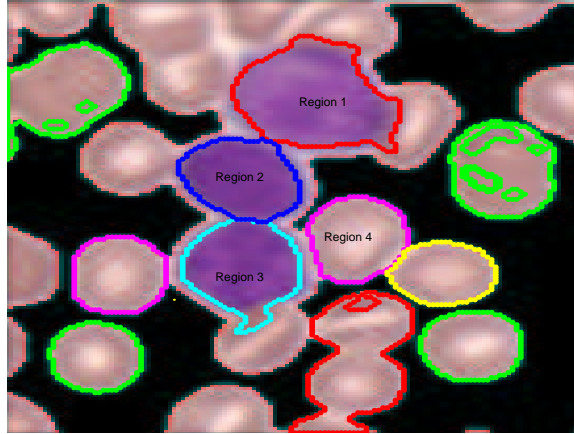


Figure 11: The regions in the central part of the image were manually separated from each other by means of "cuts". It could have been avoided by resegmenting the image with a smaller window size instead. The regions outlined in red could hypothetically be merged into one, e.g. to calculate their average intensity.

segmentation speed of color images only one or two most significant intensity/color components (as determined by singular value decomposition) could be used. From the working experience, the system has shown to be an easy to use and valuable tool in several applications. It can greatly reduce the effort spent on extraction and classification of biomedical images and which could serve as a first stage of very helpful diagnostic systems.

5 Directions for future work

At present all the advantages and disadvantages of initial image partitioning arise from the segmentation algorithm used. It will be desirable to incorporate some (prior) shape/intensity/color/texture information in its work which should lead to a more automated system. Although the latter three characteristics are somewhat easier to use (they also could be "learned" through experience with images from some particular domain), the shape information will likely require a very different segmentation algorithm, probably using the approaches from [2, 11]. The matching component of the system is also quite rudimentary but can be linked to existing finer matching algorithms if such need arises.

References

- [1] Y.Z. Cheng. Mean shift, mode seeking, and clustering. *PAMI*, 17(8):790–799, August 1995.
- [2] L. Cohen and I. Cohen. Finite element methods for active contour models and balloons for 2-d and 3-d images. *IEEE Trans. Pattern Analysis and Machine Intelligence*, PAMI-15:1133–1147, 1993.
- [3] D. Comaniciu, D. Foran, and P. Meer. Shape-based image indexing and retrieval for diagnostic pathology. In *2nd International Workshop on Statistical Techniques in Pattern Recognition*, 1998.
- [4] D. Comaniciu and P. Meer. Robust analysis of feature spaces: Color image segmentation. In *IEEE Conf. Comp. Vision Patt. Recogn.*, pages 750–755, 1997.
- [5] G. Gunter and W. S. Stiles. *Color Science – Concepts and Methods, Quantitative Data and Formulae*, chapter 13. John Wiley & Sons, Inc., 2 edition, 1982.

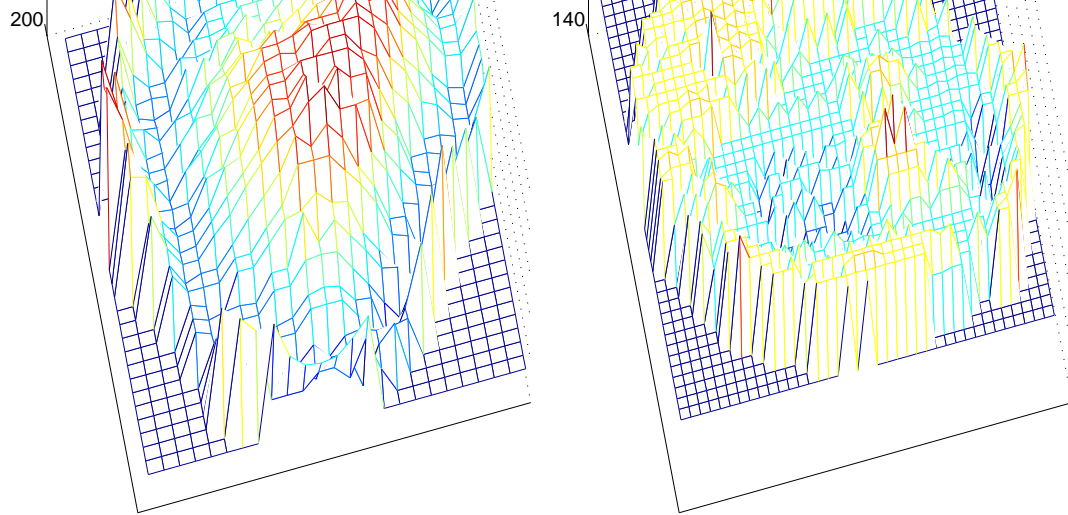


Figure 12: It is easily seen that the graphs representing regions 1 and 4 respectively of Figure 11 significantly differ in terms of their shape: This is due to the fact that the intensities of the regions.

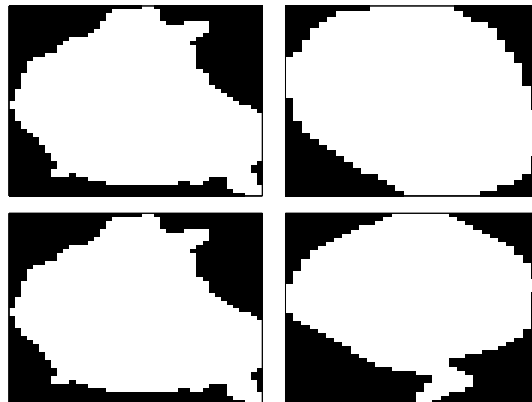


Figure 13: The top pair of images represents regions 1 and 2 of Figure 11 while the bottom pair represents regions 1 and 3 of Figure 11. The computed distance between the top pair is 2.95, and between the bottom pair is 1.67. This indicates that region 1 is "less similar" to region 2 than it is to region 3.

- [6] Stephane G. Mallat. A theory for multiresolution signal decomposition: The wavelet representation. *IEEE Trans. PAMI*, 11(7):674–693, July 1989.
- [7] E. Micheli-Tzanakou, E. Uyeda, R. Sharma, R. Ramanujan, and J. Doug. Comparison of neural network algorithms for face recognition. *Simulation*, 64(1):15–27, July 1995.
- [8] S. Sclaroff and A. Pentland. Modal matching for correspondence and recognition. *PAMI*, 17(6):545–561, June 1995.
- [9] J. Shi and J. Malik. Normalized cuts and image segmentation. In *IEEE Conf. Comp. Vision Patt. Recogn.*, pages 731–737, 1997.
- [10] Y. Wu, K. Doi, M. Giger, and R. Nishikawa. Computerized detection of clustered microcalcifications in digital mammograms: Applications of artificial neural networks. *Medical Physics*, 19(3):555–560, May/June 1992.
- [11] S.C. Zhu, T.S. Lee, and A.L. Yuille. Region competition: Unifying snakes, region growing, energy/Bayes/MDL for mutil-band image segmentation. In *Int. Conf. Comp. Vision*, pages 416–423, 1995.

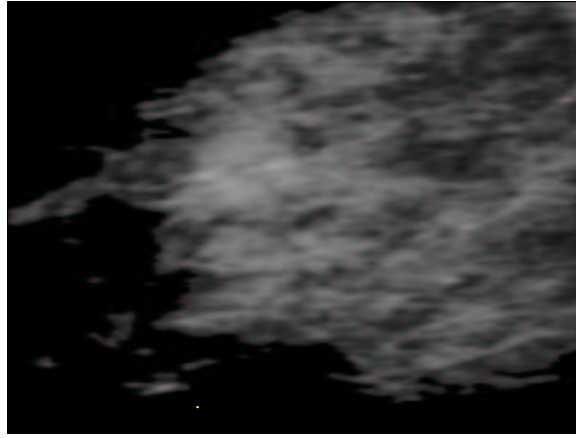


Figure 14: Original mammography image cropped and with "background" removed by prior segmentation.

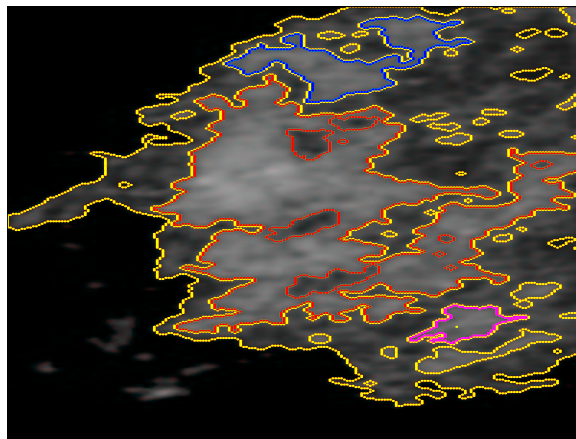


Figure 15: More precise image segmentation with probable region of interest outlined in red.

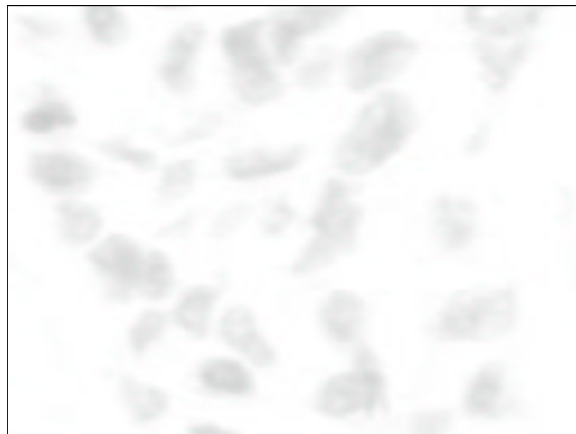


Figure 16: An image obtained from breast biopsy.

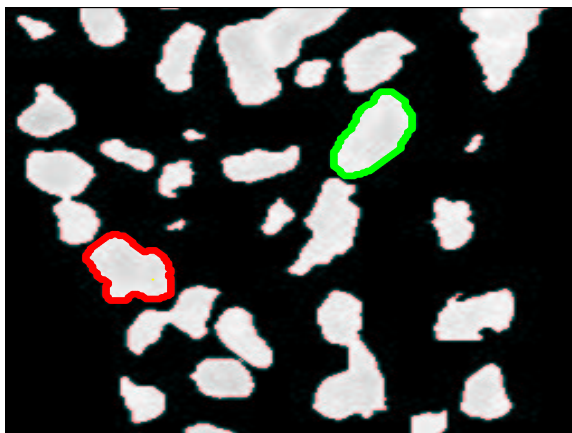


Figure 17: Breast biopsy with background removed by prior segmentation. Two sample cells are selected.

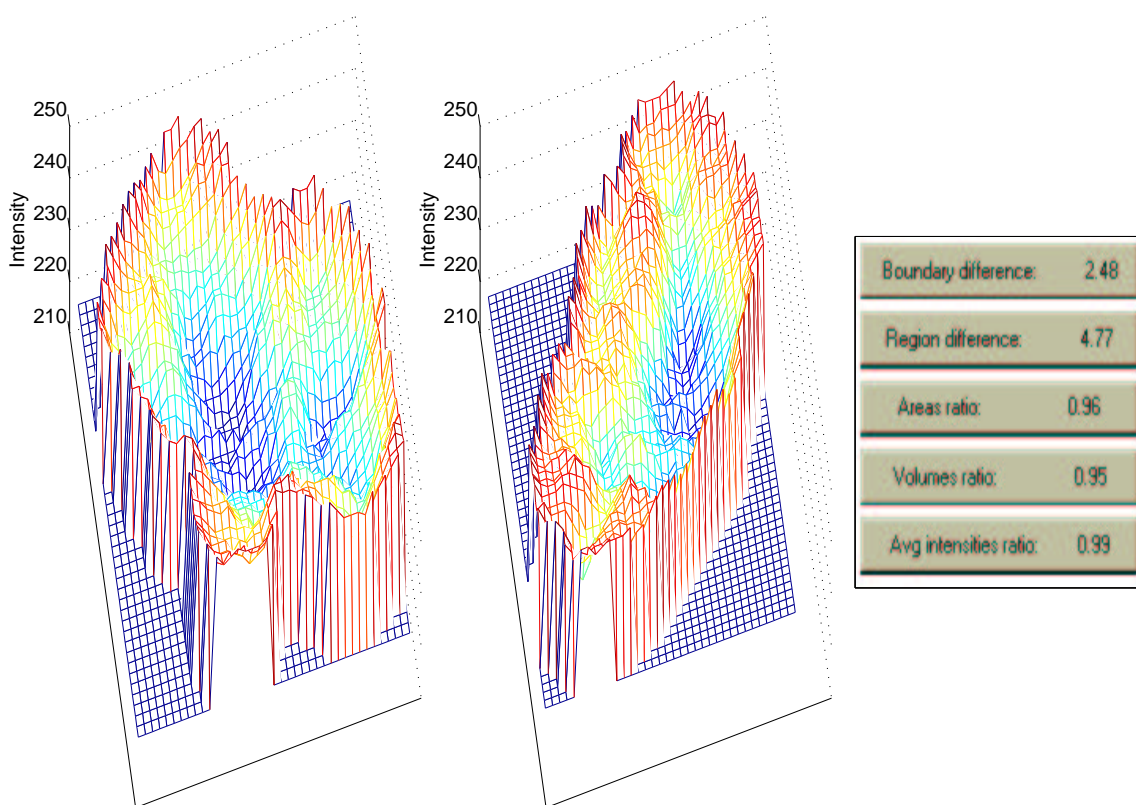


Figure 18: Representation and comparison of the selected cells.

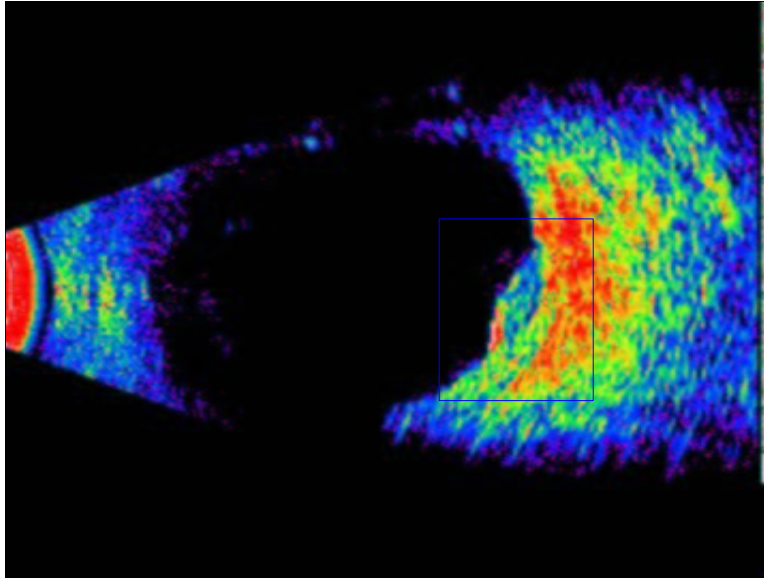


Figure 20: A color-coded image of a bird's head with a blue rectangular box highlighting a specific region on the right side.

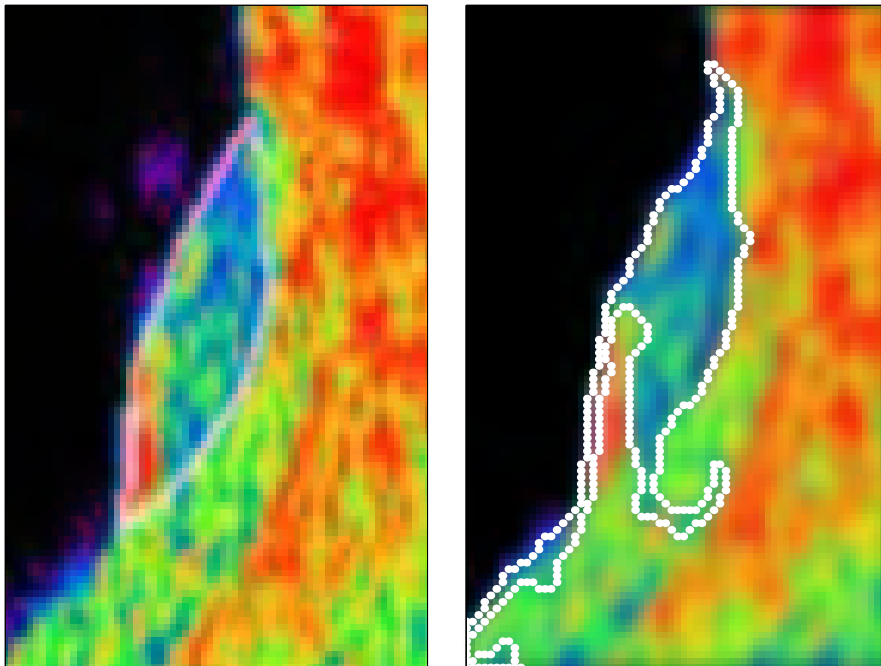


Figure 20: On the left the outline was done manually while on the right the region was found by the described methods.